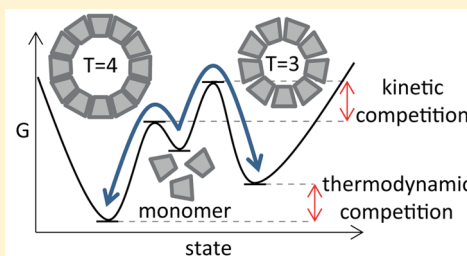


Kinetics versus Thermodynamics in Virus Capsid Polymorphism

Pepijn Moerman,^{*,†} Paul van der Schoot,^{‡,§} and Willem Kegel^{*,†}[†]Van 't Hoff Laboratory for Physical and Colloid Chemistry and [‡]Institute for Theoretical Physics, Utrecht University, 3512 JE Utrecht, The Netherlands[§]Department of Applied Physics, Eindhoven University of Technology, 612 AZ Eindhoven, The Netherlands

S Supporting Information

ABSTRACT: Virus coat proteins spontaneously self-assemble into empty shells in aqueous solution under the appropriate physicochemical conditions, driven by an interaction free energy per bond on the order of 2–5 times the thermal energy $k_B T$. For this seemingly modest interaction strength, each protein building block nonetheless gains a very large binding free energy, between 10 and 20 $k_B T$. Because of this, there is debate about whether the assembly process is reversible or irreversible. Here we discuss capsid polymorphism observed in in vitro experiments from the perspective of nucleation theory and of the thermodynamics of mass action. We specifically consider the potential contribution of a curvature free energy term to the effective interaction potential between the proteins. From these models, we propose experiments that may conclusively reveal whether virus capsid assembly into a mixture of polymorphs is a reversible or an irreversible process.



■ INTRODUCTION

The genetic material of viruses is protected by a protein shell known as the virus capsid. In the absence of the viral genome and at the appropriate pH, ionic strength, and temperature, the protein building blocks of, for example, Hepatitis B Virus (HBV), Cowpea Chlorotic Mottle Virus (CCMV), and Norwalk Virus (NV) spontaneously assemble into empty capsids in vitro.^{1–5} The main interprotein interactions driving the assembly are reasonably well-understood, as are the physical quantities that set the overall interaction strength.^{1,6} However, the propensity of virus coat proteins to assemble into a mixture of capsids of various size, known as capsid polymorphism, continues to raise debate.^{2,3,7,8} This structural polymorphism indicates that protein structure is not the only determining factor of capsid size and geometry, so the question arises what other factors may play a role. Understanding the determinants of polymorphism might be biologically relevant, because it occurs in vivo too and typically only one of the virus polymorphs is infectious.^{9–11} This suggests that antiviral strategies that tip the balance toward the formation of noninfectious polymorphs could be useful to explore.

A well-documented example of structural dimorphism in viruses is HBV, an enveloped icosahedral virus that causes infectious liver inflammation. The dimeric HBV capsid protein mutant Cp149₂ was shown to spontaneously assemble into empty virus capsids at room temperature in the absence of genome at near-neutral pH and medium to high salt concentrations.^{1,7,12,13} These capsids comprise of $T = 4$ and $T = 3$ particles in a ratio of about 95:5 almost independent of the conditions^{7,14} except at protein concentrations near the critical assembly concentration.¹³ This raises the questions what precisely determines this ratio and why it does not, or only very weakly, depend on the concentration far above the critical

association concentration. The successful description of the equilibrium between HBV capsids and monomers in terms of coarse-grained interaction energies⁶ suggests that a similar approach may be useful to describe polymorphism as well.¹⁵ Here we extend the current models describing the statics and dynamics of capsid assembly, provide an explanation for the observations and pinpoint conditions that will allow us to distinguish between kinetically and thermodynamically controlled polymorphism.

The free energy gain per virus coat protein that drives the virus capsid self-assembly process is of the order of 10–20 times the thermal energy $k_B T$.⁶ Because each protein building block makes four contacts, this implies protein–protein interactions of about 2–5 $k_B T$ per bond. This is interesting from a fundamental point of view because these bonds are not all that weak, and hence it is not a priori clear whether the spontaneous assembly and size selection of virus capsids is dominated by the rate at which they are formed (kinetics) or by the assembly free energies of the capsids (thermodynamics). In general, one can state that the distribution of capsid sizes long after the assembly reaction has terminated is either dictated by thermodynamics, when all reactions are reversible and the system can equilibrate, or by kinetics if, for example, no disassembly of completed capsids occurs.¹⁶ In the latter case, thermodynamically metastable capsids can form that are kinetically trapped.

Special Issue: William M. Gelbart Festschrift

Received: February 25, 2016

Revised: March 29, 2016

Published: March 30, 2016

Here we provide theoretical considerations on dimorphism of icosahedral viruses and address the fundamental question of whether it is governed by the thermodynamics or the kinetics of virus capsid self-assembly. The remainder of this paper is organized as follows. We first briefly review a description of the equilibrium between capsids and monomers based on the law of mass action⁶ and compare it with in vitro observed free monomer and capsid concentrations after assembly. From this analysis, we find a binding free energy per protein building block, which we later use as an input parameter in the description of polymorphism. Next, we consider competition between multiple capsid sizes by proposing two extensions to the model, one based on nucleation kinetics, and one on equilibrium thermodynamics. We compare predictions for both models with the HBV polymorphism observed in vitro and find that the free energy of assembly per monomer must depend on capsid size. Following Šiber et al., we introduce a curvature free energy term to the interaction potential between two capsid proteins.¹⁷ We find that taking this curvature free energy into account, only the model based on equilibrium thermodynamics reproduces experimental trends as a function of the coat protein concentration. At very high coat protein concentrations, where no experimental data are available, the models predict opposite trends. On the basis of this finding, we propose testable predictions that can conclusively distinguish between kinetically and thermodynamically determined polymorphism. Finally, we show that the same model also explains the absence of other capsid sizes and provide some concluding remarks.

LAW OF MASS ACTION

Let us first consider a reversible association equilibrium $nA \leftrightarrow A_n$, where protein building blocks (A) assemble into capsids (A_n) of aggregation size n . According to the law of mass action, the relation between the mole fraction x_1 of the coat protein in monomeric form and the complete capsid mole fraction x_n is given by

$$x_n = x_1^n \exp\left[-\frac{\Delta\mu_n}{k_B T}\right] \quad (1)$$

at least if the solution is ideal (that is, dilute) and incomplete capsids are present only in minute concentrations.¹⁹ Here, $\Delta\mu_n = \mu_n^0 - n\mu_1^0$ denotes the difference in chemical potential between free monomers and monomers absorbed into a capsid, which equals the gain in binding free energy upon assembly. The free energy gain arises from a hydrophobic attraction counteracted by an electrostatic repulsion between coat proteins and can be described by⁶

$$\Delta\mu_n = -A_H\gamma + A_C\sigma^2\lambda_B\kappa^{-1}k_B T + \varepsilon_C(n) \quad (2)$$

where the first term represents the hydrophobic attraction, which is the hydrophobic contact area A_H between the proteins times the surface tension γ of the protein surface with water. For HBV at room temperature, $A_H\gamma = 19 k_B T$.^{1,6} The second term gives the screened electrostatic repulsion, where A_C is the Coulombic surface area, σ is the net protein charge density, λ_B is the Bjerrum length, which is 0.7 nm at room temperature, and κ^{-1} is the Debye screening length, which obeys $\kappa^{-1} \approx \frac{0.3}{\sqrt{c_{\text{salt}}}}$ nm for a 1–1 electrolyte in water at room temperature. For HBV at near neutral pH, $A_C\sigma^2 = 1.2 \times 10^3 \text{ nm}^{-2}$.^{1,6} The last term in eq 2 is a curvature free energy that we will specify later. This term was not taken into consideration in the paper by

Kegel and Van der Schoot on account of their monodispersity approximation⁶ and we conveniently set it equal to zero for now.

The free energy of assembly given by eq 2 scales with the capsid size through the hydrophobic and electrostatic surface area. Because we want to study the competition between different capsid sizes, it makes sense to express $\Delta\mu_n$ in terms of the binding free energy per monomer ε_n so that $\Delta\mu_n = n\varepsilon_n$. Finally, we enforce conservation of mass by requiring that the total protein building block mole fraction is the sum of the mole fractions of free and absorbed monomers $x = x_1 + nx_n$ and find

$$x = x_1 + nx_1^n \exp\left[-\frac{n\varepsilon_n}{k_B T}\right] \quad (3)$$

This equation gives the monomer mole fraction as a function of total protein mole fraction for a given interaction free energy per protein building block ε_n . We can compare this with in vitro observed concentrations of HBV capsids and monomers using that the mole fraction relates to concentration c as $x = \frac{c}{55.6 \text{ M}}$ where 55.6 M is the molarity of water.

Figure 1 shows the assembly monomer, which is a protein dimer for HBV, and capsid concentrations measured by Harms

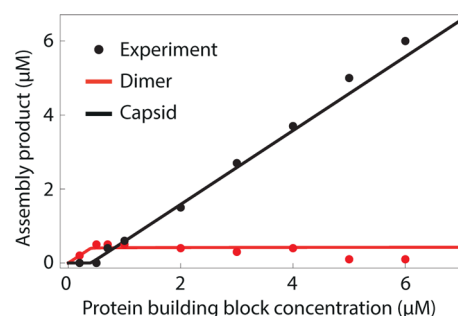


Figure 1. HBV monomer and capsid concentrations after assembly at various coat protein concentrations. Experimental data on dimer (red) and capsid (black) concentrations are used from Harms et al.¹³ The data are fitted with eq 3 using $n = 120$ (the number of dimeric protein building blocks in the HBV $T = 4$ capsid), yielding a binding energy ε_n of $-18.5 k_B T$.

et al.¹³ for HBV in an aqueous solution of pH = 7.5 and 1 M NaCl at room temperature. The red line in Figure 1 is a fit using eq 3 for $n = 120$, corresponding to an HBV $T = 4$ for the experimentally determined free monomer concentrations with ε_n as a fit parameter. The black line contains all assembly products except for free monomers and is obtained from mass conservation, $nx_n = x - x_1$. Both the experiments and curve fits show the existence of a critical association concentration, below which no assembly occurs. For large aggregation numbers n , this critical concentration is virtually independent of the exact aggregation number and only depends on the interaction free energy per monomer. Therefore, we can repeat the fit with $n = 90$ to obtain the same result, showing that polymorphism does not affect the equilibrium between monomers and capsids. In both cases, we find a binding free energy per protein building block of $-18.5 k_B T$.

Next we propose extensions to the model in order to predict the mole fractions of the different capsid sizes and we use the obtained value of $\varepsilon_n = -18.5 k_B T$ to compare the model with experimental data on HBV dimorphism. It is reasonable to use

the same value for the binding free energy because the data sets on HBV polymorphism by Zlotnick et al.¹⁴ and on HBV polymorphism and free monomer concentrations by Harms et al.¹³ were acquired at similar physicochemical conditions: room temperature in an aqueous solution with pH = 7.5 and high salt concentration, 1 and 0.8 M NaCl, respectively. Zlotnick et al.¹⁴ studied HBV dimorphism at high coat protein concentrations (24, 118, and 294 μM), and found 95% of $T = 4$ capsid using electron microscopy and 80% of $T = 4$ by sucrose gradient ultracentrifugation independent of protein concentration. We take the value of 95%, as this was also found by other studies.^{7,19} The data by Harms et al.¹³ were obtained at low protein concentrations, near the critical assembly concentration where the capsid ratio strongly varies with total protein concentration.

THERMODYNAMIC COMPETITION

If assembly is a completely reversible process and capsids continuously exchange protein building blocks to achieve an equilibrium size distribution, then the ratio between two geometrically allowed capsids is governed by the difference in their free energies. We can simply find the mole fractions of each capsid size by modifying eq 3 to allow for capsids containing p and q building blocks

$$x = x_1 + px_1^p \exp\left[-p\frac{\varepsilon_p}{k_B T}\right] + qx_1^q \exp\left[-q\frac{\varepsilon_q}{k_B T}\right] \quad (4)$$

where p and q represent the allowed aggregation numbers. These will be 90 and 120 for HBV $T = 3$ and $T = 4$ capsids, respectively. We find that if there is no curvature contribution to the interaction free energy, so that $\varepsilon_p = \varepsilon_q$, the smaller capsid is favored at all protein concentrations as is shown in Figure 2. This is because the loss of translational entropy is smaller for assembly into smaller clusters.^{17,18}

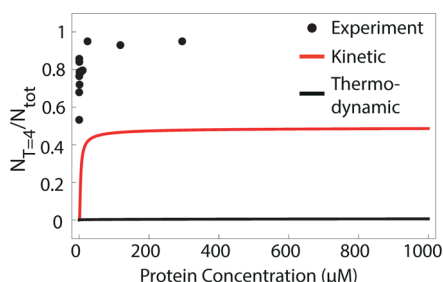


Figure 2. Both the thermodynamic (black) and kinetic (red) model predict a lower fraction of $T = 4$ capsids than is experimentally observed, when no effect of curvature is assumed. The lines are predictions from eq 4 (black) and 5 (red) using $\varepsilon_p = \varepsilon_q = -18.5 k_B T$. The black dots represent data collected from Zlotnick et al.¹⁴ and Harms et al.¹³

KINETIC COMPETITION

Alternatively, we can consider kinetic competition, where we assume reversible assembly to prevent formation of kinetically trapped intermediates, combined with strong hysteresis¹⁶ so that disassembly of complete capsids and concomitant equilibration is prohibited. This assumption is justified by the observation of subunit exchange times for HBV of the order of months.⁸ The relative number densities of the two capsid sizes will then only be determined by their respective time

dependent rates of formation, $J_p(t)$ and $J_q(t)$. Previous studies show that viral assembly is characterized by a sigmoidal increase of capsid density with time.^{20,21} We approximate this behavior with a steady-state reaction rate J^0 after a lag time t_0 such that there will be a linear increase in capsid concentration until the number of monomers reaches the critical association concentration and the capsid assembly stops.¹⁹ We compare this approach with numerical calculations that do take into account the time dependence of the assembly rate due to depletion of the monomer pool from the solution as assembly progresses and find no significant difference showing that this approximation is sensible. (See Supporting Information for more details.) Because we assumed that no disassembly can take place once the capsid is formed, the ratio between two different sizes of capsids at any time after assembly is given by

$$\frac{x_q(\infty)}{x_p(\infty)} = \frac{J_q^0(t_t - t_{0,q})}{J_p^0(t_t - t_{0,p})} \sim \frac{J_q^0}{J_p^0} \quad (5)$$

In the last step we use the fact that the lag times $t_{0,p}$ and $t_{0,q}$ are small compared to the termination time t_t , where the monomer concentration reaches the critical association concentration,²² so that a difference in lag times will not have a significant effect on the obtained dimorphism. According to classical nucleation theory of virus capsids²³ the steady-state assembly rate is given by

$$J_n^0 = \nu_n Z_n \rho e^{-\Delta G_n} \quad (6)$$

for $n = p, q$, where ν is the so-called attempt frequency that measures the inherent rate of the addition of monomers to an incomplete assembly, Z is the Zeldovich factor that is a measure for the survival time of a critical nucleus before it shrinks or grows, ρ is the concentration of free monomers at time zero, and ΔG is the free energy of nucleation scaled to thermal energy. We assume that the attempt frequency is independent of capsid size and therefore it does not influence the ratio of assembly rates in eq 5. This implies that we assume that attachment is rate-limiting. Expressions for the Zeldovich factor and the nucleation energy are given by²³

$$Z_n = \sqrt{\frac{a_n}{n\pi}} (1 + \Gamma_n^2)^{3/4} \quad (7)$$

$$\Delta G_n = \frac{n^* a_n}{2} (\sqrt{\Gamma_n^2 + 1} - \Gamma_n) \quad (8)$$

Here Γ_n is a measure of the supersaturation that drives the capsid assembly and a represents the rim energy that determines the nucleation barrier height in units of $k_B T$. These are given by the following equations²³

$$\Gamma_n = \sqrt{n-1} \left(1 - \frac{\ln(x)}{\ln(x_{c,n})} \right) \quad (9)$$

$$a_n = -\frac{\varepsilon_n}{\sqrt{n-1}} \quad (10)$$

where $x_{c,n} = \exp[\varepsilon_n/k_B T]$ is the critical association concentration, below which no assembly takes place. In principle, it depends on the size n of the capsid. Within this framework of nucleation kinetics, it is the competition between the supersaturation, favoring the formation of large capsids, and the nucleation barrier, favoring the formation of small capsids, that determines the different rates of formation and thus the dimorphism.

In order to gain insight into the consequences of this model, we investigate the limits of high and low concentration. We again take identical interaction free energies $\varepsilon_n = \varepsilon_p = \varepsilon_q$ for proteins assembling into a $T = 4$ capsid as for proteins assembling into a $T = 3$ capsid. At very low protein concentration, the supersaturation Γ_n goes to zero and the ratio x_q/x_p simplifies to $\exp\left[-\frac{1}{2}|\varepsilon_n|(\sqrt{q-1} - \sqrt{p-1})\right]$. In this limit, the ratio between $T = 4$ and $T = 3$ capsids will always be much smaller than 1, so $T = 3$ capsids are favored. If $\Gamma \gg 1$, the ratio between $T = 4$ and $T = 3$ capsids becomes 1 independent of the conditions. So, if the assembly rates set the capsid size distribution and the free energy of assembly is independent of the capsid size, then larger capsids are always disfavored or at best equally abundant as the smaller ones, as is shown in Figure 2.

CURVATURE FREE ENERGY

The above finding that smaller capsids are always more abundant if the free energy of assembly per monomer is size independent is inconsistent with numerous observations that for various mutants of the HBV capsid protein under various conditions the larger capsid is the most abundant.^{1,8,13,14,24} Therefore, we must conclude that the effective interaction free energies between proteins absorbed in capsids of different sizes is unequal. This can be understood intuitively from the fact that different capsids have different geometries so that the local interactions should be expected to vary.^{25,26} However, it is debatable whether the origin of this variation in effective interaction free energy is due to varying interaction angles that change the effective hydrophobic attraction, different protein conformations that are not equally energetically favorable, or the bending rigidity of the curved protein sheet. Although one may argue that all are merely different levels of description of an equivalent principle, we will not elaborate on the physical nature of the size-dependent free energy but just note that it is reasonable to introduce a curvature term to the free energy of interaction in eq 2 for which we invoke the following Ansatz, which was previously suggested by Prinsen et al. in a different context²⁷

$$\varepsilon_C(n) = 8\pi\kappa\left(\sqrt{\frac{n}{n_0}} - 1\right)^2 \quad (11)$$

where n_0 sets the preferred curvature of the protein and κ is the protein shell bending rigidity that sets the energy scale for the penalty related to deviation from preferred curvature. We refer to the Supporting Information for a discussion on the use of an average size dependent-free energy of binding versus a local geometry dependent-free energy. The harmonic spring character of this curvature free energy makes it general because it does not consider the source of the curvature stress. It can be shown to be isomorphic to the rotational and translational invariant curvature free energy deduced by Helfrich²⁸ that for spherical particles corresponds to

$$F_c = 4\pi R^2 \left(\frac{\kappa}{2} \left(\frac{2}{R} - \frac{2}{R_0} \right)^2 + \frac{\bar{\kappa}}{R^2} \right) \quad (12)$$

where the first term accounts for the mean curvature and the second term for the Gaussian curvature with bending elastic modulus κ and Gaussian modulus $\bar{\kappa}$. Here $1/R$ represents the capsid curvature and $1/R_0$ is the reference curvature.

Figure 3 indicates the effect of the addition of a curvature term to the free energy of interaction on the competition

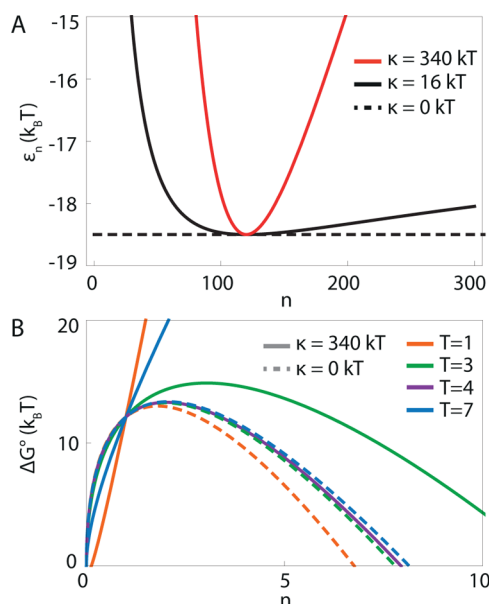


Figure 3. (A) Size-dependent free energy of interaction between coat proteins from eqs 2 and 11. The interaction energy per protein building block is shown for $\kappa = 0 k_B T$ (black, dashed), for $\kappa = 16 k_B T$ which is required to fit the thermodynamic model to the data (black, continuous), and for $\kappa = 340 k_B T$, which is required to fit the kinetic model to the data (red, continuous). In all cases $\varepsilon = -18.5 k_B T$ as found from Figure 1 and $n_0 = 120$ presuming the $T = 4$ structure to be the most stable. (B) Free energy barriers for capsid assembly with $\kappa = 0 k_B T$ (dashed) and $\kappa = 340 k_B T$ (continuous), calculated using eqs 11 from both this paper and the paper by Zandi et al.²³ The different colors refer to different capsid sizes. Note that in absence of curvature effects the smallest geometrically allowed capsid ($T = 1$) also has the lowest free energy barrier for nucleation. The addition of a curvature term, however, makes the barrier for $T = 4$ capsid formation (black line) the smallest. Again $\varepsilon = -18.5 k_B T$ and $n_0 = 120$. Note that the dashed and continuous line of the $T = 4$ capsid are on top of each other because $T = 4$ corresponds to the preferred curvature so adding a curvature term does not change the free energy of this capsid size.

between different capsid sizes. Assembly into capsids with a curvature deviating from the preferred curvature n_0 leads to a smaller gain in free energy per monomer upon assembly, as shown in Figure 3A where we set $n_0 = 120$ favoring $T = 4$ shells for dimeric coat proteins. If two competing capsid sizes exchange building blocks to obtain an equilibrium size distribution, the difference in free energy of assembly between the two capsid sizes directly sets their relative mole fractions. If the competition between capsid sizes is dictated by their respective rates of formation, the effect of the curvature free energy term is reflected in the energy barrier for nucleation as shown in Figure 3B. The height of the barrier is given by the supersaturation and by the critical nucleus size, which under experimental conditions only marginally differs between capsid sizes. For capsid sizes deviating from the preferred curvature, the decreased gain in free energy upon assembly lowers the supersaturation Γ_n , which in turn increases the barrier with respect to the situation without curvature.

Next we compare the models of thermodynamic and kinetic competition with experimental data on HBV dimorphism from Harms et al. and Zlotnick et al., this time taking the

contribution of the curvature free energy into account. Competition between the two polymorphs depends on protein concentration and through the interaction energy and the bending rigidity on temperature, salt concentration, and pH. We focus on the trends in protein concentration as this is the only parameter that does not change the bending rigidity so we can use that as a fit parameter. We assume that $n_0 = 120$ based on the experimental observation that the $T = 4$ capsid, containing 120 monomers, is the most abundant aggregate and we use the bending rigidity κ as a fit parameter, similar to the analysis by Šiber et al.¹⁷ We found that in the thermodynamic model the protein bending rigidity must be around $16 k_B T$ with a corresponding curvature free energy per protein building block absorbed in a $T = 3$ capsid of $\frac{1}{90} 8\pi 16 k_B T \left(\sqrt{\frac{90}{120}} - 1 \right)^2 = 0.08 k_B T$ in order to fit the data. For the kinetic model the required κ is $340 k_B T$ corresponding to a free energy difference per monomer of $1.7 k_B T$. These values should be low with respect to the magnitude of the original driving force because the curvature free energy is only a correction to the protein–protein interaction, and indeed they are only 0.5%, respectively 9%, of the size independent interaction free energy.

We compare the obtained values for the bending rigidity κ with literature values. Bending rigidity is a parameter in continuum elastics that sets the energy scale for a bending deformation. Direct measurements of κ are complicated by the fact that deforming virus capsids leads to local compression and expansion in addition to bending. Some estimates based on simulations and AFM measurements include $\kappa = 40 k_B T$ for Sesbania Mosaic Virus,²⁹ $\kappa = 57 k_B T$ for HK97 prohead I, $\kappa = 30 k_B T$ for prohead II,³⁰ and $\kappa = 10$ – $15 k_B T$ for HBV.³¹ Overall, the range of values for the bending rigidity that is considered generally acceptable for empty shells of viral coat proteins is 10 – $250 k_B T$.^{29–33} The $\kappa = 16 k_B T$ used for the thermodynamic model is within this range and compares well with the prediction for HBV. The bending rigidity required to fit the kinetic model is outside the range, making the thermodynamic model somewhat more plausible. However, because there is to the best of our knowledge no direct measurement of the bending rigidity of a HBV coat protein shell, we cannot exclude the possibility that polymorphism is governed by kinetics based on the required value of κ . Such measurement would conclusively reveal whether kinetics or thermodynamics are responsible for virus capsid polymorphism.

Figure 4 shows the fits of the thermodynamic and the kinetic model to the experimental data by Zlotnick et al. and Harms et al. Both models agree reasonably well with the data for higher monomer concentrations, but the steep increase in the $T = 4$ capsid fraction with increasing monomers near the critical assembly concentration is only reproduced by the thermodynamic model and disagrees with the prediction based on the kinetic model. This indicates that virus capsid polymorphism is determined by equilibrium free energies and not by kinetic trapping. Moreover, at high protein concentrations the thermodynamic and kinetic model predict opposite concentration dependencies, so measurements of the concentrations of $T = 4$ and $T = 3$ capsids at a coat protein concentration of 1 mM, where the models strongly differ, should conclusively distinguish between kinetically and thermodynamically governed polymorphism.

In the kinetic model the capsid size distribution depends on the supersaturation and through that on the protein concentration. At high protein concentrations, the super-

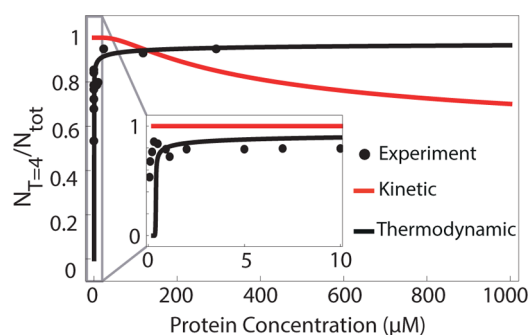


Figure 4. HBV capsid dimorphism as a function of protein concentration. The inset shows a zoom-in at low protein concentration. The circles represent the experimental data by Zlotnick et al.¹⁴ and Harms et al.¹³ The lines are fits of the kinetic (red) and thermodynamic (black) model to the data using protein bending rigidity κ as fit parameter. For the thermodynamic model $\kappa = 16 k_B T$, and for the kinetic model $\kappa = 340 k_B T$. In both cases, $n_0 = 120$ and $\epsilon_n = -18.5 k_B T$.

saturation will dominate in particular in the contribution of the rim tension and both capsid sizes will form at more or less equal rates. As a result, if dimorphism is governed by kinetics the number of $T = 3$ capsids will increase toward 50% at high protein concentrations. In the case of HBV, about 30% of the capsids should be $T = 3$ at 1 mM dimer concentration.

In the thermodynamic model, the concentration dependence comes in via the x_1^n -term in eq 1. If the total protein concentration is lower than or of the same order of magnitude as the critical association concentration, an increase in total protein concentration leads to an increase in free monomer concentration. The $T = 4$ capsid concentration scales with x_1^{120} and the $T = 3$ capsid concentration with x_1^{90} (see eq 4). So, one would expect a larger fraction of $T = 4$ capsids at higher protein concentrations. Although this effect will be weak, the concentration dependence is independent of the bending rigidity and the preferred curvature because it is purely entropic in nature. The effect will also be stronger for dimorphism between $T = 3$ and $T = 1$ capsids (with a difference of 60 building blocks) than for $T = 4$ and $T = 3$ (with a difference of 30 building blocks). Measurements on dimorphism of other viruses as a function of protein concentration could verify this.

PREFERRED CURVATURE

Another parameter that can be varied to tune dimorphism is the preferred curvature n_0 . Changing the shape of the protein would lead to a different preferred curvature and hence a different ratio between $T = 3$ and $T = 4$ capsids. Zlotnick et al.¹⁴ found that this is indeed the case. They systematically removed residues of the flexible C-terminus tail of the HBV capsid protein and found that the number density of $T = 3$ capsids increased at the expense of $T = 4$ capsids. So, apparently by varying protein construct size they tuned the preferred curvature. We can understand this qualitatively by comparing capsid formation with micellization. Long fatty acid tails lead to larger micelles (or even bilayers) because the aspect ratio between charged headgroup and hydrophobic tail is decreased and hence the preferred curvature is increased. Similarly the length of C-terminal tail (the arginine-rich motif or ARM) with respect to the size of the assembly domain of the capsid protein could be expected to affect the preferred curvature. On the other hand, the model calculations of Prinsen et al.²⁶ and Kusters et al.³⁴ indicate that the net repulsion between the

ARMs does not contribute significantly to the overall free energy of assembly. This suggests that they may play a different role, for example, by somehow influencing the molecular switching of the coat proteins required for assembly in a specific T number and hence curvature.¹⁴ What mechanism predominates remains a subject of debate.

■ GENETIC MATERIAL AND DISULFIDE BRIDGES

Other factors influencing the competition between T numbers include the coassembly of genetic material and the presence of disulfide bridges. Our model does not take the contribution of genetic material into account but studies on this topic are available from Krol et al.⁹ and Zandi et al.¹⁵ The presence of disulfide bridges alters the number of smallest building blocks and possibly the preferred curvature. We have so far only discussed protein constructs where a disulfide bridge covalently links the two proteins in a dimeric building block. Its absence would effectively double the number of assembly monomers and thus increase the contribution of entropy to the assembly process. So for these constructs we predict a larger fraction of the smaller capsid, which is in qualitative agreement with experimental findings⁸ and theory.¹⁵

■ COMPETITION WITH OTHER T -NUMBERS

The predictions presented above are based on a coarse-grained description and ignore all atomistic effects of the protein subunits. As a consequence there is a priori no reason that, within this framework, Cp149₂ should only be able to form $T = 3$ and $T = 4$ capsids and no larger or smaller capsids. If capsid polymorphism is indeed determined by a single curvature free energy term, the same free energy should account for the absence of other capsid sizes as well. Only considering icosahedral geometry, other possible capsid sizes are $T = 1$ (containing 30 protein building blocks) and $T = 7$ (containing 210 protein building blocks).³⁵ Smaller than $T = 1$ is not possible and we ignore capsids larger than $T = 7$. Using the thermodynamic model with the same value for the curvature energy as before, we found that in the range of experimental concentrations the $T = 4$ capsids are 10^{37} times more abundant than $T = 1$ capsids and 10^{24} times more abundant than $T = 7$ capsids, which is in excellent agreement with the fact that these have never been observed for HBV. In the kinetic model the suppression of other capsid sizes is less pronounced but up to 1 mM it still predicts no $T = 1$ or $T = 7$ capsids. However, at a protein concentration of 1.2 mM one would expect measurable quantities (about 1%) of the monomers to be absorbed in $T = 7$ HBV capsids. This observation would be a strong indication that HBV capsid polymorphism is determined by the kinetics instead of thermodynamics of the assembly process.

■ CONCLUSION

We find that the observed virus capsid dimorphism of HBV as well as the absence of larger and smaller capsids sizes can be explained by adding a single free energy term to the interaction potential between protein building blocks that depends on capsid size. The added free energy term has a harmonic spring character so that it is general and does not consider the source of the curvature stress. We applied this curvature term in the context of a kinetic and of a thermodynamic model to study competition between different capsid sizes. The kinetic model is valid if no monomer exchange between completed capsids occurs, thus preventing equilibration. The thermodynamic

model is valid if complete capsids do exchange monomers until equilibrium is achieved. We find that the kinetic model fails to describe the data at low protein concentration, indicating that polymorphism is governed by thermodynamics. This suggests that even complete capsids exchange building blocks and hence reach an equilibrium distribution. Furthermore, we find that at high protein concentrations the two models predict opposite trends as a function of the protein concentration. Measurements at protein concentrations of around 1 mM should conclusively reveal whether virus capsid assembly into a mixture of polymorphs is a reversible or an irreversible process.

■ ASSOCIATED CONTENT

§ Supporting Information

The Supporting Information is available free of charge on the ACS Publications website at DOI: 10.1021/acs.jpcb.6b01953.

Comparison between steady-state and time dependent rate of capsid assembly and the interaction free energy between protein building blocks in hexagonal and pentagonal symmetry. (PDF)

■ AUTHOR INFORMATION

Corresponding Authors

*(P.M.) E-mail: P.G.Moerman@uu.nl. Phone: +31 30 253 2390.

*(W.K.) E-mail: W.K.Kegel@uu.nl. Phone: +31 30 253 2873. Fax: +31 30 253 3870.

Notes

The authors declare no competing financial interest.

■ ACKNOWLEDGMENTS

We thank Jan Groenewold for fruitful discussions. This research was financially supported by the NWO Graduate Program.

■ REFERENCES

- (1) Ceres, P.; Zlotnick, A. Weak Protein-Protein Interactions Are Sufficient To Drive Assembly of Hepatitis. *Biochemistry* **2002**, *41*, 11525–11531.
- (2) Shoemaker, G. K.; van Duijn, E.; Crawford, S. E.; Uetrecht, C.; Baclayon, M.; Roos, W. H.; Wuite, G. J. L.; Estes, M. K.; Prasad, B. V.; Heck, A. J. R. Norwalk Virus Assembly and Stability Monitored by Mass Spectrometry. *Mol. Cell. Proteomics* **2010**, *9*, 1742–1751.
- (3) Lavelle, L.; Gingery, M.; Phillips, M.; Gelbart, W. M.; Knobler, C. M.; Cadena-Nava, R. D.; Vega-Acosta, J. R.; Pinedo-Torres, L. A.; Ruiz-Garcia, J. Phase Diagram of Self-Assembled Viral Capsid Protein Polymorphs. *J. Phys. Chem. B* **2009**, *113*, 3813–3819.
- (4) Gross, I.; Hohenberg, H.; Kräusslich, H. G. In Vitro Assembly Properties of Purified Bacterially Expressed Capsid Proteins of Human Immunodeficiency Virus. *Eur. J. Biochem.* **1997**, *249*, 592–600.
- (5) Cuillel, M.; Zulauf, M.; Jacrot, B. Self-Assembly of Brome Mosaic Virus Protein Initial and Final States of Aggregation Into Capsids. *J. Mol. Biol.* **1983**, *164*, 589–603.
- (6) Kegel, W. K.; van der Schoot, P. Competing Hydrophobic and Screened-Coulomb Interactions in Hepatitis B Virus Capsid Assembly. *Biophys. J.* **2004**, *86*, 3905–3913.
- (7) Wingfield, P. T.; Stahl, S. J.; Williams, R. W.; Steven, A. C. Hepatitis Core Antigen Produced in Escherichia Coli: Subunit Composition, Conformational Analysis, and In Vitro Capsid Assembly. *Biochemistry* **1995**, *34*, 4919–4932.
- (8) Uetrecht, C.; Watts, N. R.; Stahl, S. J.; Wingfield, P. T.; Steven, A. C.; Heck, A. J. R. Subunit Exchange Rates in Hepatitis B Virus Capsids Are Geometry- and Temperature-Dependent. *Phys. Chem. Chem. Phys.* **2010**, *12*, 13368–13371.

- (9) Krol, M. A.; Olson, N. H.; Tate, J.; Johnson, J. E.; Baker, T. S.; Ahlquist, P. RNA-controlled Polymorphism in the In Vivo Assembly of 180-Subunit and 120-Subunit Virions from a Single Capsid Protein. *Proc. Natl. Acad. Sci. U. S. A.* **1999**, *96*, 13650–13655.
- (10) Butan, C.; Winkler, D. C.; Heymann, J. B.; Craven, R. C.; Steven, A. C. RSV Capsid Polymorphism Correlates with Polymerization Efficiency and Envelope Glycoprotein Content: Implications that Nucleation Controls Morphogenesis. *J. Mol. Biol.* **2008**, *376*, 1168–1181.
- (11) Roseman, A. M.; Berriman, J. A.; Wynne, S. A.; Butler, P. J. G.; Crowther, R. A. A Structural Model for Maturation of the Hepatitis B Virus Core. *Proc. Natl. Acad. Sci. U. S. A.* **2005**, *102*, 15821–15826.
- (12) Freund, S. M. V.; Johnson, C. M.; Jaulent, A. M.; Ferguson, N. Moving towards High-Resolution Descriptions of the Molecular Interactions and Structural Rearrangements of the Human Hepatitis B Core Protein. *J. Mol. Biol.* **2008**, *384*, 1301–1313.
- (13) Harms, Z. D.; Selzer, L.; Zlotnick, A.; Jacobson, S. C. Monitoring Assembly of Virus Capsids with Nano-Fluidic Devices. *ACS Nano* **2015**, *9*, 9087–9096.
- (14) Zlotnick, A.; Cheng, N.; Conway, J.; Booy, F. P.; Steven, A. C.; Stahl, S. J.; Wingfield, P. T. Dimorphism of Hepatitis B Virus Capsids Is Strongly Influenced by the C-terminus of the Capsid Protein. *Biochemistry* **1996**, *35*, 7412–7421.
- (15) Zandi, R.; van der Schoot, P. Size Regulation of ss-RNA Viruses. *Biophys. J.* **2009**, *96*, 9–20.
- (16) Singh, S.; Zlotnick, A. Observed Hysteresis of Virus Capsid Disassembly is Implicit in Kinetic Models of Assembly. *J. Biol. Chem.* **2003**, *278*, 18249–18255.
- (17) Šiber, A.; Majdandžić, A. Spontaneous Curvature as a Regulator of the Size of Virus Capsids. *Phys. Rev. E* **2009**, *80*, 021910.
- (18) Castelnovo, M.; Muriaux, D.; Faivre-Moskalenko, C. Entropic Control of Particle Sizes during Viral Self-Assembly. *New J. Phys.* **2013**, *15*, 035028.
- (19) van der Schoot, P.; Zandi, R. Kinetic Theory of Virus Capsid Assembly. *Phys. Biol.* **2007**, *4*, 296–304.
- (20) Zlotnick, A.; Johnson, J. M.; Wingfield, P. W.; Stahl, S. J.; Endres, D. A. Theoretical Model Successfully Identifies Features of Hepatitis B Virus Capsid Assembly. *Biochemistry* **1999**, *38*, 14644–14652.
- (21) Chen, C.; Kao, C. C.; Dragnea, B. Self-Assembly of Brome Mosaic Virus Capsids: Insights from Shorter Time-scale Experiments. *J. Phys. Chem. A* **2008**, *112*, 9405–9412.
- (22) Hagan, M. F.; Elrad, O. M. Understanding the Concentration Dependence of Viral Capsid Assembly Kinetics - The Origin of the Lag Time and Identifying the Critical Nucleus Size. *Biophys. J.* **2010**, *98*, 1065–1074.
- (23) Zandi, R.; van der Schoot, P.; Reguera, D.; Kegel, W. K.; Reiss, H. Classical Nucleation Theory of Virus Capsids. *Biophys. J.* **2006**, *90*, 1939–1948.
- (24) Newman, M.; Suk, F.; Cajimat, M.; Chua, P. K. Stability and Morphology Comparisons of Self-Assembled Virus-Like Particles from Wild-Type and Mutant Human Hepatitis B Virus Capsid Proteins. *Journal of Virology* **2003**, *77*, 12950–12960.
- (25) Mannige, R. V.; Brooks, C. L. Geometric Considerations in Virus Capsid Size Specificity, Auxiliary Requirements, and Buckling. *Proc. Natl. Acad. Sci. U. S. A.* **2009**, *106*, 8531–8536.
- (26) Bruinsma, R.; Gelbart, W.; Reguera, D.; Rudnick, J.; Zandi, R. Viral Self-Assembly as a Thermodynamic Process. *Phys. Rev. Lett.* **2003**, *90*, 248101.
- (27) Prinsen, P.; van der Schoot, P.; Gelbart, W. M.; Knobler, C. M. Multishell Structures of Virus Coat Proteins. *J. Phys. Chem. B* **2010**, *114*, 5522–33.
- (28) Helfrich, W. Elastic Properties of Lipid Bilayers — Theory and Possible Experiments. *Z. Naturforsch. C* **1973**, *28*, 693–703.
- (29) May, E. R.; Brooks, C. L. Determination of Viral Capsid Elastic Properties from Equilibrium Thermal Fluctuations. *Phys. Rev. Lett.* **2011**, *106*, 188101.
- (30) May, E. R.; Brooks, C. L. On the Morphology of Viral Capsids: Elastic Properties and Buckling Transitions. *J. Phys. Chem. B* **2012**, *116*, 8604.
- (31) Nguyen, T. T.; Bruinsma, R. F.; Gelbart, W. M. Elasticity Theory and Shape Transitions of Viral Shells. *Phys. Rev. E - Stat. Nonlinear, Soft Matter Phys.* **2005**, *72*, 1–53.
- (32) Roos, W. H.; Gibbons, M.; Arkhipov, A.; Uetrecht, C.; Watts, N. R.; Wingfield, P. T.; Steven, A. C.; Heck, A. J. R.; Schulten, K.; Klug, W. S.; Wuite, G. J. L. Squeezing Protein Shells: how Continuum Elastic Models, Molecular Dynamics Simulations, and Experiments Coalesce at the Nanoscale. *Biophys. J.* **2010**, *99*, 1175–1181.
- (33) Klug, W. S.; Bruinsma, R. F.; Michel, J.; Knobler, C. M.; Ivanovska, I. L.; Schmidt, C. F.; Wuite, G. J. L. Failure of Viral Shells. *Phys. Rev. Lett.* **2006**, *97*, 1–4.
- (34) Kusters, R.; Lin, H.; Zandi, R.; Tsvetkova, I.; Dragnea, B.; van der Schoot, P. Role of Charge Regulation and Size Polydispersity in Nanoparticle Encapsulation by Viral Coat Proteins. *J. Phys. Chem. B* **2015**, *119*, 1869–1880.
- (35) Caspar, D. L. D.; Klug, A. Physical Principles in the Construction of Regular Viruses. *Cold Spring Harbor Symp. Quant. Biol.* **1962**, *27*, 1–24.